A Perceptually Adaptive Scheme for Image Watermarking by Bit Inverting Transformation

Tadahiko Kimoto
Faculty of Science and Engineering
Toyo University
Japan
kimoto@toyonet.toyo.ac.jp

***ABSTRACT**: A perceptually adaptive scheme for image watermarking by use of the bit inverting transformation is developed. The transformation can change a signal level by both inverting a specified bit and altering the level at random within a limited range. From the analysis of the transformation properties, a perceptual model with two kinds of measures of level distortion is assumed for evaluating subjective visual qualities of the transformed image. Using the measurements of visual quality by the subjective evaluations of human observers, the subjective quality measure based on the perceptual model is derived by multiple linear regression analysis. This measure can estimate a subjective visual quality from the two distortion measurements of the transformed image.*

In the adaptively watermarking scheme, by using the subjective quality measure, the embedding parameter is adaptively determined every image block so that a desired visual quality can be achieved on the resulting watermarked image. The simulation results demonstrate the performance of the subjective quality measure and the efficiency of the adaptively watermarking scheme.

Keywords: Digital Watermark, Spatial Domain, Subjective Image Quality, Perceptual Model, Multiple Linear Regression Analysis, Perceptually Adaptive System

Received: 26 December 2010, Revised 28 January 2011, Accepted 4 February 2011

1. Introduction

Digital watermarking is a technique for embedding additional signals, so-called watermarks, into digital signals such as images and afterward extracting them [1]. From the viewpoint of the domain to embed watermark signals into, the watermarking techniques are mainly divided into two categories: spatial-domain-based techniques and transform-domain-based ones.

In the watermarking of images, the transform-domainbased techniques can usually provide not only good visual quality in the resulting images but also stronger robustness against image modification than the spatial-domain-based ones. However, it is hard to embed watermarks exactly into transform domains. In the case of image watermarking, the pixel values of a source image, which are the quantized levels or integers, are first transformed into frequencies. The frequency coefficients are then modified so as to represent watermarks. The values inversely transformed from such modified transform domain are usually real numbers with fractions. Thus, the quantization errors occur inevitably when the integral spatial domain is reconstructed. These errors are likely to disturb the watermark existing in the transform domain.

In contrast, exact watermark signals can be embedded into the spatial domain, though they are fragile under signal modification. The traditional method for spatial-domainbased image watermarking is first to select pixels in a source image and then, to modify the levels of the selected pixels so that the watermark can be expressed there [2]. The most primitive method for

modifying a pixel level is to select a bit in the binary expression of the level and then, to invert the selected bit [3]. In this method, the bit position selected in the binary expression as well as the pixel location selected in a source image must be kept secret so that the watermark can be protected from unauthorized access.

The embedded watermark distorts the source signal to some extent. The transformation in the image spatial domain has especially direct effects on visual quality. In the bit inverting method, inverting the *k*th bit, denoted by bit-*k*, where the 0th bit is the least significant bit, changes the signal level by 2^k. Hence, the visual distortion caused by the level change increases with an increase in *k*. On the other hand, when a bit-*k* holds a watermark bit, an attacker searches some range of integers for the correct value of *k* to obtain the bit-*k*. With increasing *k*, the searching range becomes larger, and accordingly, a tolerance to unauthorized access increases. Hence, a method for evaluating visual quality of the watermarked image is necessary to implement the embedding of watermark efficiently.

In the previous papers, we have proposed a method for inverting a bit-*k* while reducing the level change less than or equal to 2^{k-1} [4][5]. Suppose that a source level is allowed to change by up to 2^{k-1}. Then, some additional signal-transformation as well as the inverting of the bit*k* can be performed. As such additional transformations, we have considered the randomly changing of signal levels [6]. Or alternatively, if the pixels of inverted bits are to be discriminated in the watermark extraction side, additional watermark bits can be embedded there [7].

In the present paper, we develop a scheme for implementing the bit inverting transformation to embed watermark bits so that a desired subjective visual quality can be achieved on the resulting image. For this purpose, we consider the randomly changing of signal levels as the additional signal transformation above mentioned. Then, a perceptual model for evaluating visual quality of the watermarked images is constructed based on the human visual system [8]. Such a perceptual model is a function of objective quality measures that can approximate human subjective quality. Variouskinds of quantities are proposed for the measurement of objective quality [12]. In the modeling here, the quantities based on the properties of the bit inverting transformation are defined for the objective quality measures. By determining adaptively the embedding parameters by means of the perceptual model, the watermarking scheme can perform as a *perceptually adaptive system* [9].

In Section II we outline the signal transformation including the inverting of signal bits, and describe the properties of the distortion caused by the transformation. In Section III we consider the modeling of subjective quality of the transformed images. First, two kinds of objective quality measures are defined from the properties of the distortion. Then, using the measurements of subjective quality, we determine the subjective quality measure by multiple linear regression analysis. In Section IV the scheme for adaptively implementing the transformation is developed by using the subjective quality measure. The performance of the scheme is demonstrated in the simulation result. Furthermore, the validity of the subjective quality measure is considered. Finally, Section V concludes the paper.

2. Bit Inverting Transformation

2.1 Bit Inverting with Level Compensation

The inverting of a bit of a signal results in a change of the signal level. The signal level is supposed to be uniformly quantized to *M* bits and expressed from the *M*-bit sequence of 0···0 to that of 1···1 in natural binary. Each bit in the binary expression is denoted by bit-*k* for $k = 0, 1, \ldots, M-1$, and bit-0 means the least significant bit. Also, let $B(v, k)$ denote the binary value of bit-*k* of the signal level *v*. The inverted bit-*k* changes, that is, either increases or decreases the signal level by 2^k. The amount of the level change can be reduced by altering the other bits of the signal.

The bit conversion that performs both the inverting of bit-*k* in an *M*-bit signal and the minimizing of the resultant level change is expressed in the following level transformation $g_{M,k}$ from v_s to v_B: letting $\Delta_k = 2^{k-1}$ and, for simplicity in notation, $n = \lfloor v_S/\Delta_k \rfloor$ where $\lfloor x \rfloor$ denotes the integral part of the real number *x*,

$$v_B = g_{M,k}(v_s) = \begin{cases} (n+1)\Delta_k, & \text{if } n \text{ is even} \\ n\Delta_k - 1, & \text{if } n \text{ is odd} \end{cases}, \qquad (1)$$

where $0 \le v_s \le 2^M - 1$, for $n = 0, 1, \ldots, 2^{M-k+1} - 1$. Here, as described later, $k \ge 1$. Figure 1 shows the input-output relationship of the transformation by the bold lines.

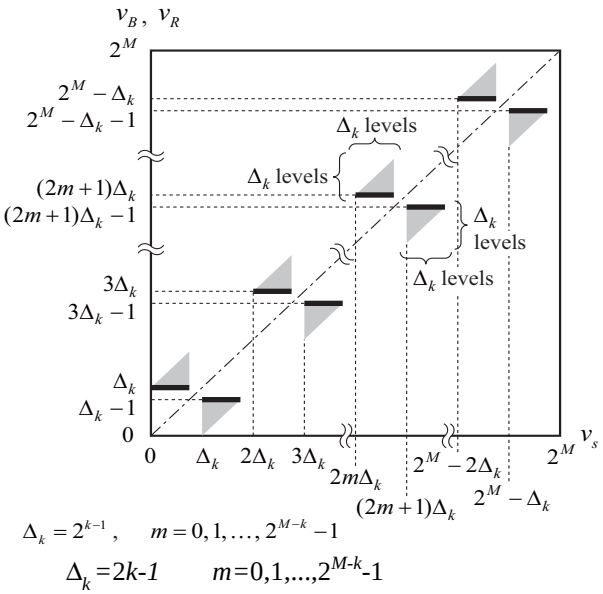

Figure 1. Input-output relationship of the level transformations: the bold lines represent $v_B = g_{M,k}(v_s)$; the shaded areas represent the ranges of $v_R = h_{M,k}(v_s)$

The relationship between the input level v_s and the output level $v_B = g_{M,k}(v_s)$ has the following properties:

(a) Concerning the values of bit-(k-1),

$$B(v_B, k\text{-}1) = \overline{B(v_s, k\text{-}1)} \tag{2}$$

where $\bar{b}$ denotes the 1's complement of a bit b.

(b) Concerning the values of bit-k,

$$B(v_B + \Delta_k, k) = \overline{B(v_B + \Delta_k, k)} \tag{3}$$

where adding Δ_k is carried out in modulus of 2^M.

(c) v_B is closest to v_s in those levels that satisfy (3). That is,

$$|v_B\text{-}v_s| = \min_{v} \{|v\text{-}v_s| \; B(v + \Delta_k, k) = \overline{B(v_s + \Delta_k, k)}\} \tag{4}$$

The level change caused by $g_{M,k}$ depends on the input level as Figure 1 shows. Letting $d_{M,k}(v) = g_{M,k}(v)\text{-}v$, for $0 \le v_s \le 2^M\text{-}1$,

$$\begin{cases} 1 \le d_{M,k}(v_s) \le \Delta_k, & \text{if n} = \lfloor vs/\Delta_k \rfloor \text{ is even} \\ -\Delta_k \le d_{M,k}(v_s) \le -1, & \text{if n is odd} \end{cases} \tag{5}$$

Thus, it is the bit-(k-1) that is inverted in the signal, and the inversion of bit-k is performed in the levels shifted by 2^{k-1}. Consequently, a signal of any level in the input dynamic range changes by 2^{k-1} levels or below with the bit-k inverted. This performance holds for $1 \le k \le M\text{-}1$. Hence, $g_{M,k}$ has been defined in this range of k.

2.2 Level Randomization

The transformation $g_{M,k}$ maps 2^M consecutive source levels into 2^{M-k+1} sparse output levels. Hence, the resulting images look like coarsely quantized ones. The transformed levels can be distributed in the same range as the input dynamic range by a stochastic process. Taking into account that the maximum change caused by $g_{M,k}$ in the source dynamic range is Δ_k levels, we transform the output $v_B = g_{M,k}(vs)$ further to v_R so that it can satisfy both of the following two conditions:

(i) The inversion of bit-k is achieved;

$$B(v_R + \Delta_k, k) = \overline{B(v_s + \Delta_k, k)} \quad (6)$$

(ii) The amount of level change remains Δ_k or below;

$$|v_R - v_s| \leq \Delta_k. \quad (7)$$

The above v_R is obtained by adding an appropriate random level to v_B. The procedure is as follows: Let $v_B = g_{M,k}(v_s)$ and $n = \lfloor vs/\Delta_k \rfloor$.

Step 1: Calculate the range w where v_B can change at random.

$$w = \begin{cases} v_s \leq \Delta_k - v_B, & \text{if n is even} \\ v_B - (v_s - v_k), & \text{if n is odd} \end{cases} \quad (8)$$

Thus $0 \leq w \leq \Delta_k - 1$.

Step 2: Let r be an arbitrary level in the range $[0, w]$.

Step 3: v_R is obtained by altering v_B by r in the following manner:

$$v_R = \begin{cases} v_B + r, & \text{if n is even} \\ v_B - r, & \text{if n is odd} \end{cases} \quad (9)$$

Considering the above procedure to be a level transformation from v_s to v_R, let $v_R = h_{M,k}(v_s)$. $h_{M,k}(v_s)$ is a stochastic function whose range depends on vs as below:

$$\begin{cases} v_R \in [\, g_{M,k}(v_s), v_s + \Delta_k \,], & \text{if n is even} \\ v_R \in [\, (v_s - \Delta_k, g_{M,k}(v_s)], & \text{if n is odd} \end{cases} \quad (10)$$

The number of levels composing the output range varies in $[1, \Delta_k]$. Hence, the randomization is achieved for $k \geq 2$.

Figure 1 includes the input-output relationship of $h_{M,k}$ by showing the stochastic output ranges by the shaded areas. Thus, the range of $h_{M,k}$ spreads all over the M-bit dynamic range.

2.3 Watermarking by Using Transformation

In this section, a use of the transformation $h_{M,k}$ for image watermarking is specified. Consider the embedding of a watermark into a cover image by merely substituting each watermark bit for a certain bit of a pixel.

Let X denote a cover image composed of $N_x \times N_y$ pixels, and $X(x, y)$ be the pixel level at the coordinates (x, y) in X for $x = 0, 1, \ldots, N_x$ and $y = 0, 1, \ldots, N_y$. W denotes a watermark that is a sequence of ordered L bits $\{w_0, w_1, \ldots, w_{L-1}\}$, where $L \leq N_x \times N_y$.

1) Embedding procedure: The procedure for embedding the whole W into X is described as follows:

Step 1: Select L different points $p_i = (x_i, y_i)$ within X for $i = 0, 1, \ldots, L-1$. Let P denote the sequence of the ordered L points $\{p_0, p_1, \ldots, p_{L-1}\}$.

Step 2: Assign an integer k_i in the range $[2, M-1]$ to each point pi for $i=0, 1, \ldots, L-1$. Let K denote the sequence of the ordered L integers $\{k_0, k_1, \ldots, k_{L-1}\}$.

Step 3: Modify the pixel level at the point $pi = (x_i, y_i)$ in X so that the k_ith bit can represent w_i, for $i = 0, 1, \ldots, L-1$. Let $v_s = X(x_i, y_i)$ and $b_s = B(v_s + \Delta_{ki}, k_i)$. The pixel level is transformed from v_s to v_{out} by the following relation:

$$v_{out} = \begin{cases} h_{M,k}(v_s), & \text{if } b_s \neq w_i \\ v_s, & \text{if } b_s = w_i \end{cases} \quad (11)$$

As a result of the above procedure, the watermarked image, denoted by X', is obtained. Both P and K must be kept from those

who have no permission to extract the watermark.

2) Detection procedure: To extract the watermark from the watermarked image *X'*, the steps listed below can be used:

Step 1: Obtain both *P* and *K* associated with *X'* .

Step 2: At the point $p_i = (x_i, y_i)$ in *X'*, the watermark bit w_i is extracted by

$$w_i = B(X'(x_i, y_i) + \Delta_{ki}, k_i) \quad (12)$$

for $i = 0, 1, ..., L\text{-}1$

Thus, the whole of the watermark *W* is given by the sequence of the extracted bits $\{w_0, w_1, \ldots, w_{L-1}\}$.

2.4 Properties of Transformation

1) Change of signal levels: The output level $v_R = h_{M,k}(v_s)$ is a random variable, and accordingly, the level difference of v_R and v_s ,written by $d_R = v_R - v_s$, also changes at random. The range of the random change is determined for each v_s as shown in Figure 2.

2) Change of level occurrences: The difference in width among the ranges of $h_{M,k}(v_s)$ affects the occurrence of the output level v_R. We have analyzed the occurrence frequencies of v_R under both the assumption that *M*-bit input levels are uniformly distributed over the dynamic range and the assumption that v_R is chosen in the output range with the uniform probability distribution. The analysis result is shown in Figure 3.

Although the output range of $h_{M,k}$ spreads over the entire *M*-bit range, in every two ranges of Δ_k levels the order of two ranges are reversed through the mapping, as shown in Figure 4. These reversed ranges result in distortions on the picture surface.

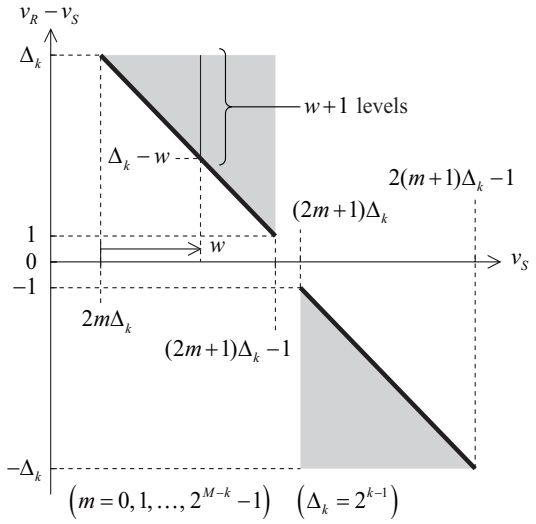

Figure 2. Relationship between input level and level difference: $v_R = h_{M,k}(v_s)$.
Bold lines just represent the level difference caused by $g_{M,k}(v_s)$

2.5 Image Distortions

The distortions caused by $h_{M,k}$ have two phases. In the first phase that is caused by $g_{M,k}$, although the change in each signal level is made minimum, the number of levels available in the image is reduced. The second phase is caused by the level randomization. In this phase the number of levels appearing in the image increases while the change from the source image increases accordingly. Each phase of distortion affects the image quality in different manners.

1) Distortion in low-detail regions: The first phase of the distortion affects especially the quality of low-detail image regions. Figure 5 shows examples of the transformations of an 8-bit grayscale ramp image with $k = 5$. In Figure 5(b) we may perceive eight *stairs*, which can be referred as *false contours*, in the gradation transformed by $g_{M,k}$, while the image actually has 16 different stairs.

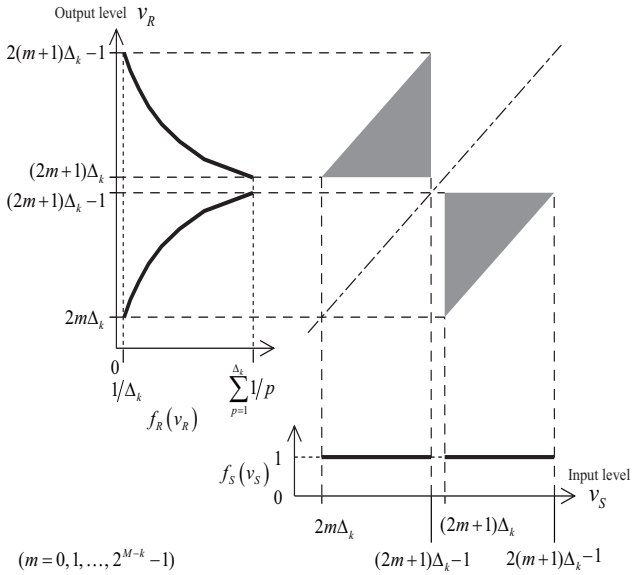

Figure 3. Output level occurrence distribution of $h_{M,k}$ obtained in the stochastic analysis

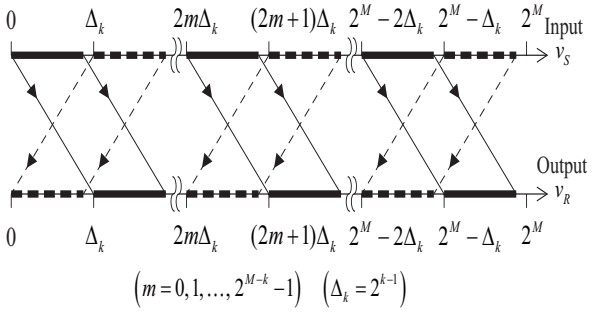

Figure 4. Correspondence of $h_{M,k}$ between input and output levels

Figure 5(c) shows the randomized version of Figure 5(b). The false contours of the random levels in Figure 5(c) look half as wide as those in Figure 5(b). Note that an extremely large value of *k* has been used in Figure 5 so that the distortion is certainly visible.

Image size: 256 by 128 pels
Leftmost level: 0 (black)
Rightmost level: 255 (white)
Level gradient is 1 level/pel

(a)

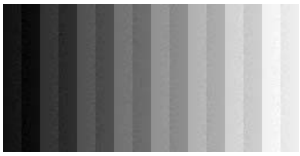

(b) (c)

Figure 5. Transformed images of a grayscale ramp ($M = 8$, $k = 5$): (a) A source ramp; (b) The result of $g_{M,k}$ consisting of 16 levels; (c) The result of $h_{M,k}$ consisting of 256 levels

2) Distortion in high-detail regions: We consider a local image area where source levels are bounded in a small range. If the source level range is $[2m\Delta_k, 2(m+1)\Delta_k)$, the transformed levels lie in the same range, as Figure 3 has shown. On the contrary, if the source range of $2\Delta_k$ levels is $[(2m+1)\Delta_k, (2m+3)\Delta_k)$, the transformed levels lie outside the range and no levels appear inside the range (Fig. 6(a)). If the source range of $3\Delta_k$ levels is $[(2m+1)\Delta_k, 2(m+2)\Delta_k)$, there also exists an empty range where no transformed levels appear (Figure 6(b)). Both the replacement of ranges and the missing ranges cause distortions in the texture of the local areas.

3. Perceptual Modeling

3.1 Objective Quality Measures

The level transformation $h_{M,k}$ causes distortion in the source image, and thus, degrades the image quality. According to the performance analysis of $h_{M,k}$, we have defined two kinds of objective measures to evaluate the distortion.

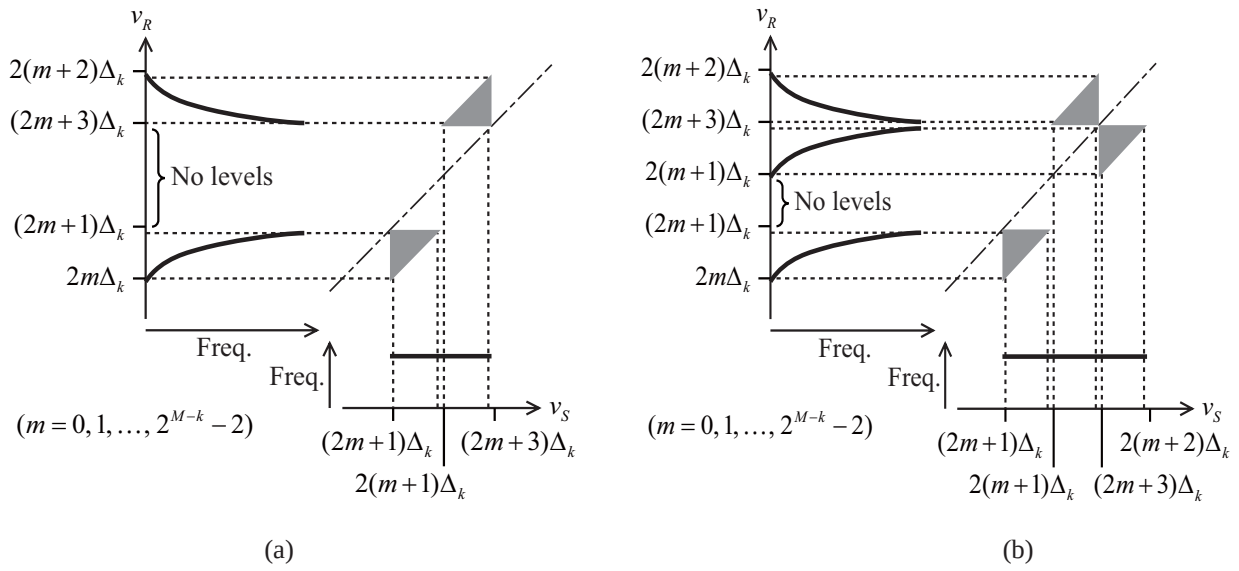

Figure 6. Transformation $h_{M,k}$ from bounded source ranges: Source levels are assumed to occur uniformly in the range

1) Change of signal levels: The first measure is the mean-square-difference (MSD) between two images. The MSD between a source image *X* and the transformed image *X'* , denoted by *D*msd, is defined by

$$D_{\text{msd}} \triangleq \frac{1}{N_x N_y} \sum_{y=0}^{N_y-1} \sum_{x=0}^{N_x-1} (p'_{x,y} - p_{x,y})^2 \qquad (13)$$

where $p_{x,y}$ and $p'_{x,y}$ are pixel levels at the coordinates (x, y) in *P* and *P'*, respectively, for $x = 0, 1, ..., N_{x-1}$ and $y=0, 1,..., N_{y-1}$. The MSD of a watermarked image (or region) evaluates the mean distortion over the whole image (or region).

2) Change of level occurrence distributions: By $h_{M,k}$ in every interval of $2\Delta_k$ levels in the input dynamic range, the upper half and the lower half are mapped inversely into the output dynamic range, as already shown in Figure 4. To evaluate the change in the level occurrence distribution, we define the square variation of level occurrence between a source image *X* and the transformed image *X'*, denoted by

D_{dst}, by

$$D_{\text{dst}} \triangleq \sum_{i=0}^{2^M-1} (f'_i - f_i)^2 \Big/ \sum_{i=0}^{2^M-1} f_i^2 \qquad (14)$$

where f_i and f'_i are the relative occurrence frequencies of a signal level *i* in the picture *X* and *X'*, respectively, for $i = 0, 1, ...,2^M-1$, satisfying $\sum_{i=0}^{2^M-1} f_i = 1$ and $\sum_{i=0}^{2^M-1} f'_i = 1$.

3.2 Subjective Testing

To find a correlation between the objective quality and the subjective quality of the transformed images, we have carried out the subjective evaluations by human observers [10]. In the measurement of image quality, we used a *ratingscale* method [11] where the observers viewed the test images and assigned each image to one of the given ratings. The results were presented by computing a mean value from the numerical values corresponding to the ratings, which is referred to as a Mean Opinion Score (MOS).

The testing materials were prepared in the following way. Here, assuming that M =8, that is, we have only considered 8-bit images.

• $h_{M,k}$ was implemented with a pseudo-random number generator of a computer in the stochastic process.

• The test images were printed on photographic papers in 200 pels per inch with a **PICTROGRAPHY**-3500 printer, which has a printing resolution of 400 dots per inch.

All the observers, who were all in their twenties, were unfamiliar with the performance of $h_{M,k}$. They were asked to look at the materials sitting at a desk under ceiling lights inside a room.

Two kinds of source images were used. The first one is a 256-grayscale ramp image where the pixel levels vary linearly from 0 to 255 extending from the top side to the bottom side. Thus, the ramp image represents a low-detail region. The transformation $h_{M,k}$ makes the linear gradation of levels distorted in the output image. Accordingly, transforming the source ramp with varying both the value of k and the ratio of pixels chosen to transform in the image, which is referred as the transformation ratio τ, yields the distorted images of various values of D_{msd}. In the measurement of subjective quality each test image was not compared with the source image, but evaluated from a viewpoint of the appearance of smooth gradation and assigned one of the five ratings of the absolute rating scale listed in Table I(b).

The other kind of source image was a granular image representing a high-detail region. The source images used in the measurement were composed of pixels of (pseudo-) random levels ranging uniformly in bounded intervals of a width of a multiple of Δ_k levels for a given k. According to the stochastic analysis of the mapping characteristics, the transformed images have the same D_{msd} (more strictly, almost same D_{msd} with a small difference due to the pseudorandom numbers) and the different D_{dst} depending on the source intervals. Samples of the test images are shown in Figure 7. Each transformed image was compared with the source image just printed beside on the same paper and then, evaluated according to the degree of perceptible difference with the impairment rating scale listed in Table I(a).

Thus, eleven scores were collected for each test image, and the MOS was calculated from them.

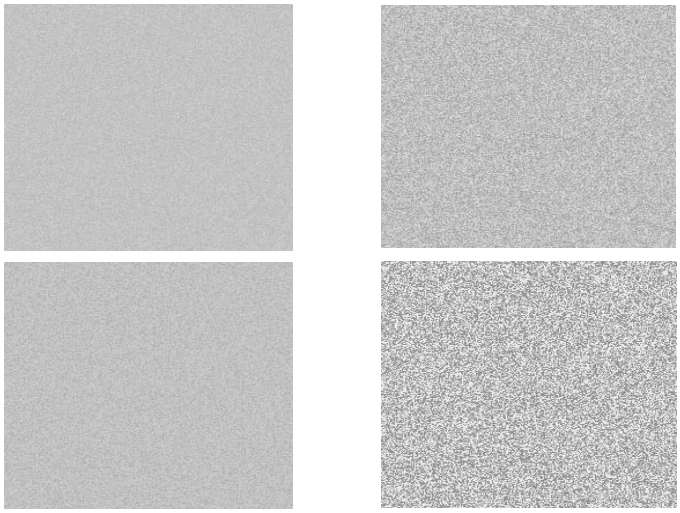

(a) (b)

Figure 7. Samples of the pairs of a source image and the transformed image that were used for comparative testing in the subjective evaluation: (top) source images of the levels spatially located at random and uniformly ranging in the interval of (a) $[23\Delta_4, 26\Delta_4)$ and (b) $[5\Delta_6, 7\Delta_6)$; (bottom) the corresponding transformed images with (a) $k = 4$ and (b) $k = 6$. All the images are shown at 200 pixels/inch here

3.3 Subjective Quality Measure

In the evaluation of the ramp images, a subjective quality of each test image of a different Dmsd value was measured in MOS. Figure 8 shows the measured MOS S_{mos} plotted against D_{msd} calculated by (13). The result indicates an approximately linear

correlation between the subjective quality and the logarithms of D_{msd}. Consequently, *D*msd has the primary effect on the estimation of MOS for the images transformed by $h_{M,k}$.

Value	Rating
5	Imperceptible
4	Perceptible but not annoying
3	Slightly annoying
2	Annoying
1	Very annoying

(a)

Value	Rating
5	Excellent
4	Good
3	Fair
2	Poor
1	Bad

(b)

Table 1. Ratings Used in the Subjective Testing

In the evaluation of the granular images, those test images transformed with the same k have the same D_{msd} and the different D_{dst}. Figure 9 shows the measured MOS plotted against the D_{dst} calculated by (14) for k = 3, 4, 5 and 6. For a given k, the MOS values S_{mos} decrease as the D_{dst} increases. We suppose that the correlation between *S*mos and D_{dst} can be considered approximately linear, while the gradients vary with the value k.

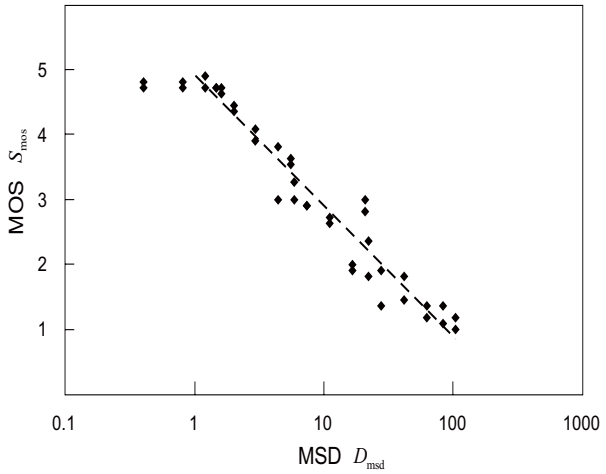

Figure 8. Measurements of subjective image qualities MOS versus level change D_{msd}: The broken line shows the linear regression line in the middle range of $1 \leq D_{msd}$. Note that the abscissa is on a log scale

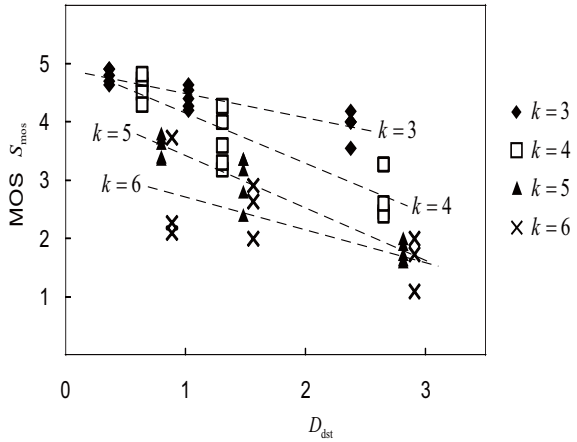

Figure 9. Measurements of subjective image qualities MOS versus level occurrence change D_{dst}: The broken line shows the linear regression line for each k

For a transformed image region, let us consider a subjective quality measure as a function of two parameters, D_{msd} and D_{dst}, that estimates a subjective quality of the distortion, where D_{msd} and D_{dst} are measured by comparing the distorted image with the source image. According to the above analysis of the measurements, we suppose that a subjective quality measure S_{mos} can be expressed as a linear combination of the logarithm of D_{msd} and D_{dst}. That is,

$$S_{mos} = \alpha . \ln D_{msd} + \beta . D_{dst} + \gamma \quad (15)$$

where α, β and γ are parameters to be estimated by multiple linear regression analysis.

To carry out the regression analysis, we used the triplets of $\{S_{mos}, D_{msd}, D_{dst}\}$ measured from the test granular images described above. Thus, 54 measurements of the dependent variable *S*mos at 12 different values of the independent variable vector (D_{msd}, D_{dst}) were used in the multiple linear regression analysis. As a result, the values of α, β and γ are estimated as

$$\hat{\alpha} = -0.46, \hat{\beta} = -0.70 \text{ and } \hat{\gamma} = 6.4, \quad (16)$$

respectively. Also, the resulting coefficient of determination, which is commonly denoted by R^2, is 0.86. Figure 10(a) shows the correlation between the values of S_{mos} predicted with the parameter values of (16), S_e, and the measured values. Thus, the subjective quality measure S_e gives the values comparable to the MOS values.

To evaluate the effect of D_{dst} on the modeling of S_{mos}, we have also used a simple linear regression model of one independent variable of D_{msd}. In this model, S_{mos} is expressed in the form

$$S_{mos} = \alpha' . \ln D_{msd} + \beta . D_{dst} + \gamma' \quad (17)$$

where α' and γ' are the model parameters. By using the same data as those used in the above multiple regression analysis, these two parameters were estimated from 54 measurements of *S*mos at four different values of D_{msd} in simple linear regression analysis. As a result, we obtained the estimated values of α' and γ' as

$$\alpha' = -0.55 \text{ and } \gamma' = 5.7, \quad (18)$$

respectively. Also, the resulting value of R^2 was 0.55. The values of S_{mos} predicted by this model are compared to the measured values in Figure 10(b). The relation between the measured and predicted values of S_{mos} in Figure 10(a) has higher correlation than that in Figure 10(b). Thus, D_{dst} as an independent variable improves the linear model of S_{mos}.

4. Perceptually Adaptive Watermarking

4.1 Block Processing Procedures

The subjective quality measure S_e gives an estimate of subjective quality for each image region under the assumption that the whole of the region is transformed with a given value of *k*. Let $S_e(k)$ denote the value of S_e under the transformation with *k*.

Figure 11 shows an example of values of the subjective quality measure with various *k*, where the measure is applied to every non-overlapping block of 4×4 pixels in a source grayscale image. It is observed that the measure values vary for a given *k* according to the image texture. Also, the measure values tend to increase with decreasing *k*.

By using the subjective quality measure S_e, we can examine whether the transformation of an image region with a value of *k* satisfies a given condition of subjective quality. Accordingly, the measure can determine the values of *k* to transform an image region with so that the desired subjective quality can be achieved. Because the level range available for the additional transformation extends with increasing *k*, the largest one of the available *k*'s is to be chosen. Furthermore, the value of *k* to use can be changed for each image region.

To implement the above adaptive watermarking, we determine both a threshold value S_T comparable to the subjective quality measure and an upper limit of available *k*, which is equal to *M*-1 here. The S_T can be determined from the ratings listed in Table I. Here, let us assume the transformation ratio is 1. Then, the value of *k* for each image region, k_B, is determined by

$$k_B = \max_{1 \le k \le M\text{-}1} \{k \mid S_e(k) \ge S_T\}. \quad (19)$$

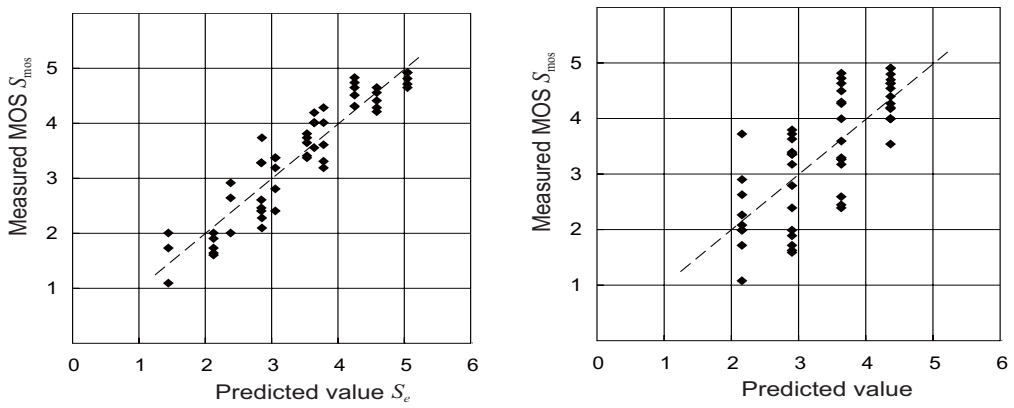

(a) (b)

Figure 10. Measured values *S*mos and calculated values S_e: The broken line shows the linear regression line for these plotted points

The region is actually transformed with k_B. Thereby, the subjective image quality of $S_e(k_B)$ is achieved in the transformed region.

The procedure for implementing (19) is carried out in each image region, starting from $k = 1$ as follows:

Step 1: Transform the region with the value of k.

Step 2: Calculate D_{msd} by (13) and D_{dst} by (14) within the region.

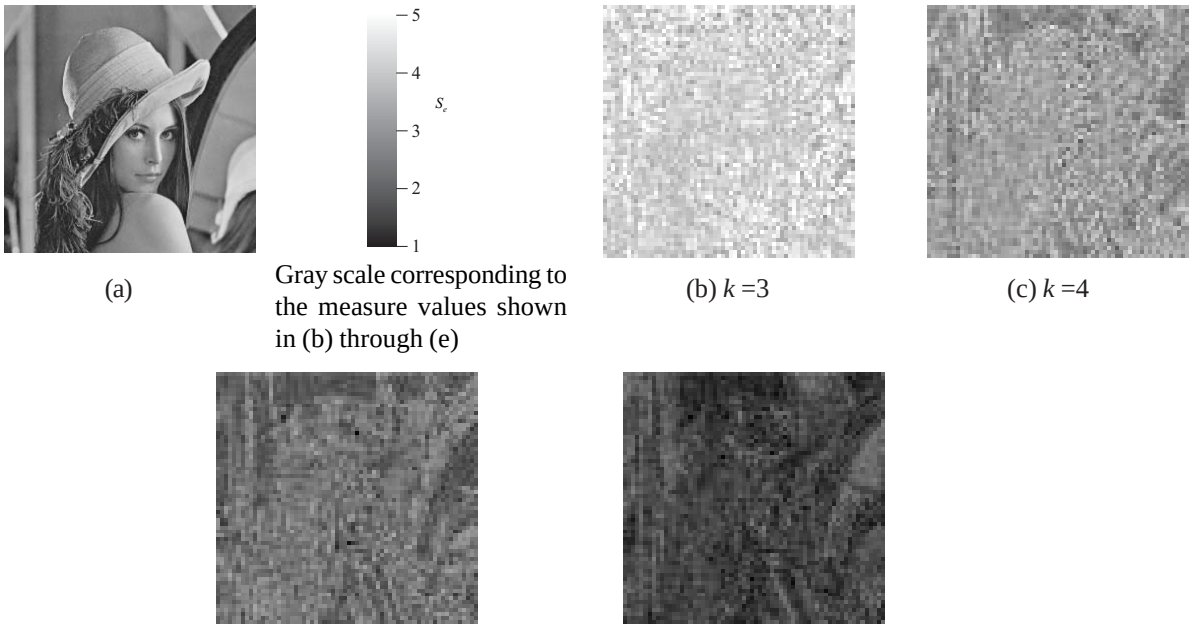

(a) Gray scale corresponding to the measure values shown in (b) through (e) (b) k =3 (c) k =4

(d) k =5 (e) k =6

Figure 11. Examples of values of the subjective quality measure. (a) Source imageN 'Lena' of 256×256 8-bit pixels. (b)-(e) Grayscale images showing the measure values $S_e(k)$ applied to 4×4-pixel blocks. The average is (b) $\overline{S}_e(3) = 4.3$, (c) $\overline{S}_e(4) = 3.5$, (d) $\overline{S}_e(5) = 2.7$, and (e) $\overline{S}_e(6) = 2.1$

Step 3: Calculate $S_e(k)$ as S_e of (15) with the specified coefficients of (16).

Step 4: Compare $S_e(k)$ with the given S_T. If $S_e(k) < S_T$, $k_B = k$-1. Otherwise, increase k by one, and repeat from *Step 1*.

4.2 Simulation Results

Simulations of the adaptive watermarking were carried out. The test images of 256×256 8-bit pixels, which are well known as 'Lena', 'Peppers', 'Cameraman' and so on, were used as the source images. The adaptively watermarking procedure was implemented every block of 4×4 pixels in the simulation with various threshold value S_T.

Figure 12 shows an example of the values of the parameter k_B that were determined for each block by the adaptive scheme. From this figure it is observed that the adaptive scheme performs such that in the low-detail regions such as the 'sky', where the human visual system is sensitive to distortion [11], k_B's of small values are assigned, and in the high-detail regions such as the lower half of the image k_B's of large values can be used.

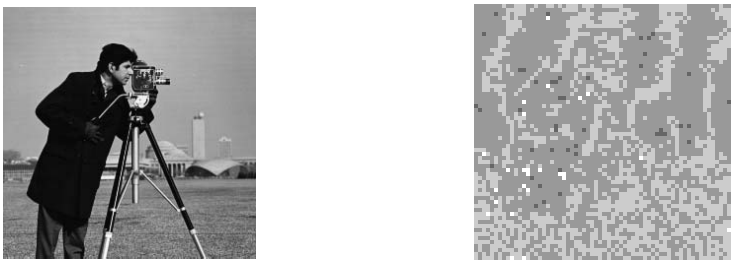

(a) Source 'Cameraman' (b) k_B values

Figure 12. The embedding parameters k_B that are determined for each block by the adaptive scheme: Block size is 4×4 pels and the threshold S_T = 3.5. In (b), black means k_B = 1, and the brighter, the larger k_B

Table II shows for the source image 'Peppers' the distribution of the values of k_B that were determined by the adaptive scheme for various S_T .With increasing S_T the ratios of large k_B's decreases, and the average of k_B decreases accordingly.

Table II also shows the value of S_e averaged over all the blocks in the image. As this result indicates, the averaged value of S_e was achieved at about 0.5 greater than the given threshold for each of the images in the simulation. The reason why this difference is likely to occur is considered that only integers are available for k.

The block size is 4×4; Source image 'Peppers'.						
		Threshold S_T				
		3.0	3.5	4.0	4.5	5.0
Number of blocks (%)	k_B = 1	0	0	0	2.3	44.6
	k_B = 2	0	0.68	18.7	67.5	52.2
	k_B = 3	7.7	54.3	74.9	30.0	3.2
	k_B = 4	71.0	44.5	6.5	0.07	0
	k_B = 5	21.3	0.51	0	0	0
	k_B = 6	0.07	0	0	0	0
Averaged k_B		4.14	3.45	2.88	2.28	1.59
$\overline{S_e}$		3.60	4.10	4.54	4.99	5.46
PSNR (dB)		30.3	34.0	37.3	40.6	44.2

Table 2. Simulation Result of Percetually Adaptive Watermarking

Examples of the images resulting from the same source image for S_T = 3.0, 4.0 and 5.0 are shown in Figure 13. From these images it is observed that the better visual quality is certainly achieved as the threshold quality S_T is set larger.

2.3 Validity of Subjective Quality Measure

We consider the validity of the subjective quality measure in this section. When we look at an image, we usually evaluate the quality of the whole image. Taking account of this fact, we compare the subjective quality measure to human evaluations in terms of the whole image quality.

(a) Source 'Peppers'

(b) S_T = 3.0; $\overline{S_e}$ = 3.60, PSNR=30.3 dB

(c) S_T = 4.0; $\overline{S_e}$ = 4.54, PSNR=37.3 dB

(d) S_T = 5.0; $\overline{S_e}$ = 5.46, PSNR=44.2 dB

Figure 13. Results of the adaptive watermarking with the various threshold values S_T : Each right column image magnifies a 64 by 64 pel region of the left one, whose size is 256 by 256 pels

Using various images produced in the simulation of the adaptive scheme, first, we have carried out the subjective evaluations of visual quality by use of the impairment rating scale listed in Table I. The MOS value S_{mos} was then obtained from the scores of about forty people for each image, who were given no information about the making of the images. Note that these S_{mos}'s are the evaluation of the whole image quality. Next, to estimate subjective quality of the whole image from a collection of the measure values of block quality, the block values S_e were averaged over all the blocks in each image, and the mean value $\overline{S_e}$ is obtained.

Figure 14 shows the relationship between the mean value $\overline{S}_e$ and the measured S_{mos} in each of the three test images. A linear correlation between S_{mos} and $\overline{S}_e$ is clearly observed from either result in this figure. However, the slope of the linear regression line is 1.9, 1.8 and 2.2 in Figure 14(a), (b) and (c), respectively.

This inclined linear correlation results in the incorrect prediction of subjective quality by the measure as that, for example, viewers evaluate the quality of an image at the worst MOS of one, while the mean value of block quality indicates that the image holds the quality of MOS of three.

The value $\overline{S}_e$ can be corrected using the corresponding value of S_{mos} by linear regression analysis. The linear regression model is expressed in the form

$$S_{mos} = \mu \cdot \overline{S}_e + v \tag{20}$$

where μ and v are to be estimated by simple linear regression analysis. To carry out the analysis, we collected the pairs of $\{\overline{S}_e, S_{mos}\}$ where $1 \leq \overline{S}_e \leq 5$, from the results of three images shown in Figure 14. As a result, the parameters μ and v are estimated as

$$\hat{\mu} = 1.9, \text{ and } \hat{v} = -4.4, \tag{21}$$

respectively.

Using (21), the values of $\overline{S}_e$ in Figure 14 were modified to $\overline{S}_e$. The resulting relationship between S_{mos} and $\overline{S}_e$' is shown in Figure 15. In this figure, each value of S_{mos} is shown with its 95% confidence interval. The slope of any linear regression line in the figure is about 1.1. Furthermore, from the viewpoint of the confidence intervals of MOS, the linear correlation looks valid. Consequently, $\overline{S}_e$' can be used to predict the evaluation of subjective quality for at least these three images.

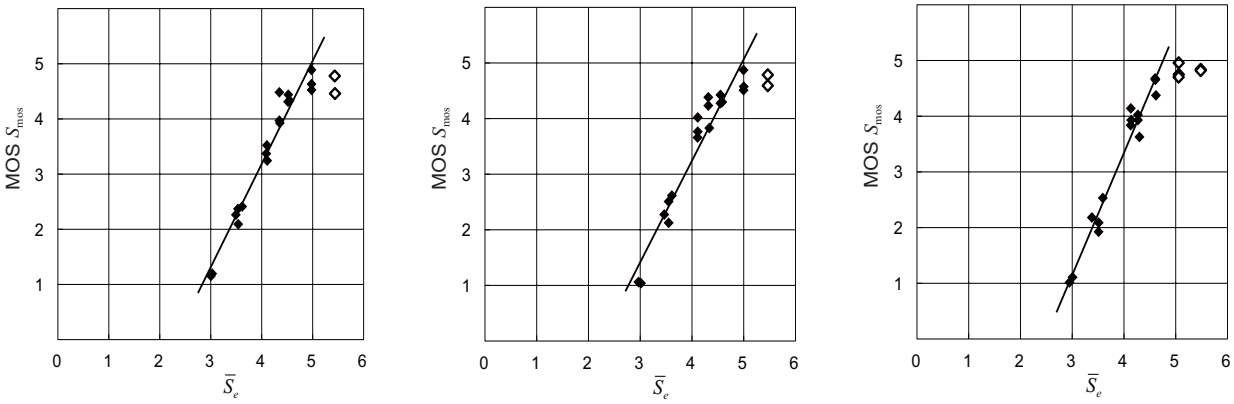

(a) Image 'Lena' (b) Image 'Peppers' (c) Image 'Cameraman'

Figure 14. MOS versus the subjective quality measure averaged over the blocks $\overline{S}_e$ for each source image used in the simulation. The line in each figure shows the linear regression of the data points. The points painted solid in white are out of range $1 \leq \overline{S}_e \leq 5$

5. Conclusion

The properties of the subjective quality measure, which is the primary result in this paper, are summarized below:

• The subjective quality measure is the function of two objective quality measures, D_{msd} and D_{dst}, obtained from an image region. Consequently, the subjective quality measure is essentially carried out in block processing.

• The subjective quality measure predicts a value of MOS in the impairment rating scale. Hence, a threshold value for the measure values can be given in terms of subjective evaluation.

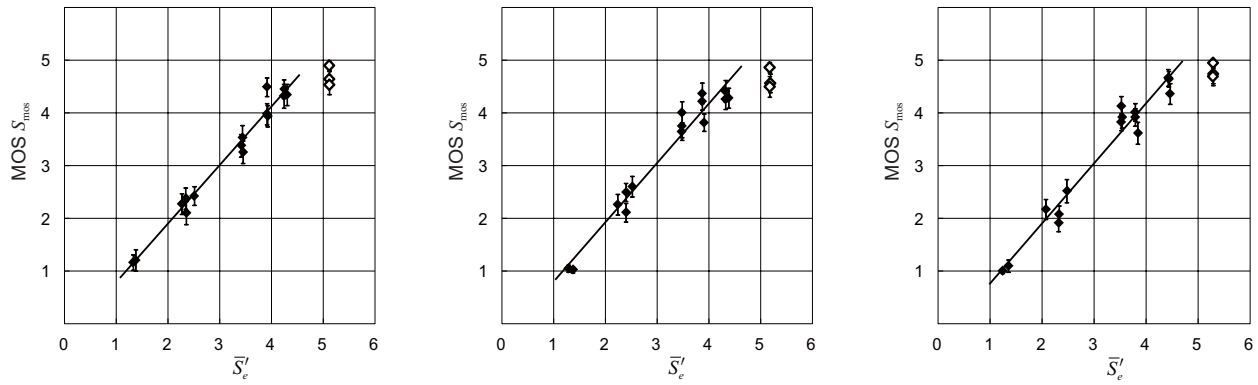

(a) Image 'Lena' (b) Image 'Peppers' (c) Image 'Cameraman'

Figure 15. MOS versus the modified $\overline{S}'_e$ for each source image used in the simulation. The line in each figure shows the linear regression of the data points. The points painted solid in white are out of range $1 \leq \overline{S}'_e \leq 5$

• The values of the subjective quality measure are dependent both on the bit position to be inverted and on the image texture. This property enables the bit position to vary depending on the image texture in the adaptive scheme.

On the other hand, the subjective quality measure was derived from the measurements of the computer synthesized test patterns. The validity of the measure for natural scene images was examined in terms of the whole image quality. We obtained the whole image quality value by averaging the block quality value over the blocks within the image. In the experiment using three test images, a highly but inclined linear correlation was observed between the mean value and the measured MOS. Although the inclined gradient was successfully corrected by simple linear regression analysis in this experiment, the cause of the difference between the estimated values and measured values of whole image quality may be related to human eye's characteristics [11]. Accordingly, we have to consider a method for estimating the whole image quality from the block qualities in more detail.

Another remaining subject is the block size of the subjective quality measure. The block size of 4×4 has been used in this paper. The block size is related to the resolution of quality measure. On the other hand, a bit position to be inverted is decided at each block in the adaptive scheme. Hence, the same number of bit positions as the blocks must be preserved and afterward provided for the extraction procedure. From these viewpoints, the appropriate block size should be considered.

References

[1] Macq, B.M. ed. (1999). Special issue on identification and protection of multimedia information. *Proc. of IEEE* , 87 (7) 1059–1276.

[2] Wang, F.H., Pan, J.S., Jain, L.C. (2009). Innovations in Digital Watermarking Techniques. Springer-Verlag Berlin Heidelberg.

[3] Oka, K., Matsui, K. (1997). Signature method into grayscale images with embedding function. *IEICE Transactions on Information and Systems* J80-D-II (5) 1186–1191 (in Japanese).

[4] Kimoto, T. (2005). Implementation of level transformations for hiding watermarks in image bit-planes under limited level changes. *In: Proc. of the IEEE International Conference on Image Processing (ICIP 2005)* , pages 253–256. Genova, Italy, Sept.

[5] Kimoto, T. (2007). Modified level transformation for bit inversion in watermarking. *In: Proc. of the IEEE International Conference on Image Processing (ICIP 2007)* . San Antonio, USA, Sept.

[6] Kimoto, T. (2006). A sophisticated bit-conversion method for digital watermarking. *In: Proc. of the 8th IASTED International Conference on Signal and Image Processing* , pages 139–144. Honolulu, USA, Aug.

[7] Kimoto, T. (2009). An advanced method for watermarking digital signals in bit-plane structure. *In: Proc. of IEEE International Conference on Communications (ICC 2009)* , SPCP2.8. Dresden, Germany, June.

[8] Awrangjeb, M., Kankanhalli, M.S. (2004). Lossless watermarking considering the human visual system. *In: Digital watermarking*, pages 581–592. Kalker, T., Cox, I.J., Ro, Y.M. eds (2004). Springer.

[9] Cox, I.J., Miller, M.L., Bloom, J.A. (2002). Digital watermarking. Morgan Kaufmann Publishers.

[10] Mikami, D., Shimizu, M., Makabe, S., Kamiyoshihara, Y., Kimoto, T. (2008). Measurement of subjective quality of watermarked images made by inverting bits. *In: Proc. of IEEE TENCON 2008 (TENCON2008)* , O17-7. Hyderabad, India, Nov.

[11] Netravali, A.N., Haskell, B.G. (1988). Digital Pictures. Plenum Press, New York, USA.

[12] Wang, Z., Bovik, A.C., Sheikh, H.R., Simoncelli, E.P. (2004). Image Quality Assessment: From Error Visibility to Structural Similarity. *IEEE Transactions on Image Processing* 13 (4) 600–612.

Author Biography

Tadahiko Kimoto received the B.E., M.E. and Dr. E. degrees in electronic engineering from the University of Tokyo, Japan, in 1980, 1982 and 1992, respectively. After graduating from the graduate school of the University of Tokyo in 1986, he was with the University of Tokyo. He moved to Waseda University in 1993, and then, moved to Nagoya University in 1994. Since 2002, he has been with Toyo University, where he is now a professor of the Faculty of Science and Engineering. His research interests span a wide range of topics in computer image system and human visual systems.